September 2024

Analytic Validation: MALDI-Glycan – Version 1.0
Stanford University CIMAC

Performance Lab:
Bendall / Angelo Lab
Sean Bendall, PhD
1291 Welch Road
Edwards building, R139
Stanford, Palo Alto, CA, 94305

Table 1. Summary of analytical validation findings for MALDI-Glycan

Accuracy:	Glycan mass matching 20ppm or better; 0.002Da per 1000Da (**Figure 8)**
Precision:	Intra-assay precision: Absolute signal +/- 14%; Mass Accuracy better than 20ppm, Correlation R^2 = 0.998. See **Figures 7-8**;
Analytical sensitivity:	Variable > ~10^4 copies per pixel (50um)
Analytical specificity	N-Linked Glycans Library Constructed *In Silico*. Predicted Structures Confirmed by Chemical and Enzyme Specificity (**Figures 2 and 3**)
Reportable range	N-Glycan mass library with masses ranging from 700-4000 m/z (~Da)
Standardization, Reproducibility	Reproducibility – Independent Quadruplets (**Figure 4-7**)
Other Performance Data	Dynamic range and linearity: up to 10^3 on a per pixel basis Sample stability over time: Samples here were sectioned at the same time and processed and acquired > 1 month period

Introduction.

The analysis of *N*-glycan distributions in formalin-fixed, paraffin-embedded (FFPE) tissues by matrix-assisted laser desorption/ionization (MALDI) imaging mass spectrometry (IMS) is an effective approach for characterization of many disease states (**Figure 1**). The workflow has matured over years of optimized protocols (1-15) and new technology has emerged; approaches are needed to more efficiently characterize the isomeric structures of these *N*-glycans to expand on the specificity of their localization within tissue. Sialic acid chemical derivatization (**Figure 2**) can be used to determine the isomeric linkage (α2,3 or α2,6) of sialic acids attached to *N*-glycans, while endoglycosidase F3 (Endo F3, **Figure 3**) can be enzymatically applied to preferentially release α1,6-linked core fucosylated glycans, further describing the linkage of fucose on *N*-glycans.

Here we describe the performance and validation of workflows where *N*-glycans are chemically derivatized to reveal sialic acid isomeric linkages, combined with a dual-enzymatic approach of endoglycosidase F3 and PNGase F to further elucidate fucosylation isomers on the same tissue section. This is adapted from work published by colleagues at MUSC(1). Now, the Stanford CIMAC has performed additional reproducibility and robustness assessments of the N-Glycan MALDI assay on sequential FFPE archival tissues (**Figure 4**).

Human kidney is a highly structured tissue that contains some of the most diverse and differentially abundant glycan structures. Therefore, to assess the robustness and reproducibility of the N-glycan assay at the Stanford CIMAC we performed 4 independent serial analyses on FFPE human kidney. Serial sections of kidney were independently processed according to the established N-Glycan analysis workflow according to Figure 1, Appendix I. Samples were processed and imaged on independent days. The resulting MALDI mass spectra peaks were matched against a database of theoretical glycan structures (16). Data was extracted in parallel and raw extracted peak intensities were used for all calculations and analysis here.

Results.

Serial N-Glycan Analysis Yields Qualitatively Similar Glycan Imaging Patterns that are Similar to H&E Staining Pattern

The resulting spatially resolved mass spectra generated for these serial MALDI-N-Glycan samples were matched against a library of almost 300 possible glycoforms. Over 100 glycoforms were identified here across all samples. Overall, glycan imaging patters yield a distribution of patterns that is consistent with the observed H&E staining pattern for a serial section of the same kidney tissue (**Figure 5**, *Top*) Qualitative assessment of glycan imaging patters (**Figure 5**, *Bottom*)) shows consistent, and inverse, expression patterns for H5N4F1 and H5N5F1, demonstrating the consistency of the assay and the ability of glycan expression to coincide with differential tissue biology / regions.

Signal Variation in the MALDI N-Glycan Assay Variation is Unimodal.

Given that individual N-glycan peaks displayed qualitatively similar distribution patters across tissues (**Figure 5**) we wanted to assess how a larger set of assigned N-Glycan peaks co-vary. **Figure 6** shows the co-variation of the top (~1/3) of the expressed N-Glycans identified across the 4 replicate kidney samples. The *Top* bar graph shows the raw extracted peak intensities for each independent replication (*Bar color*). Looking across the individual glycan peaks (x-axis) it was observed that the relative variation of peak intensity was consistent across samples where sample 2>4>1>3 had the greatest to least intensity. Ratiometric assessment of this variability (**Figure 6**, *Bottom*) showed that the variation was quite consistent from peak to peak. Taken together, these data indicate that while data was largely consistent, signal variation was largely unimodal likely due to small changes in instrument sensitivity or enzyme performance generating analyte from run-to-run.

The Stanford CiMAC MALDI N-Glycan Assay is Robust and Highly Correlated between Replicates.

Given the unimodal nature of signal variation from run to run we anticipated that the larger dataset would have a high degree of correlation between independent replicates. To this end, Pearson Correlation Analysis was performed across the intensities of the top 100 glycoforms identified across all replicates (**Figure 7**). Expected, the intensity values across all peaks were highly correlated (R^2 average 0.998) with the large variation seen in the slope (Average 0.992 with an S.D. of 0.16, or 14%). This higher standard deviation is reflected in the unimodal signal shifts (**Figure 6**) which were still largely consistent between independent runs. The extremely high intensity correlation combined with slope variation observed reinforces the unimodal nature in assay signal variation and is a strong indicator that standard, linear multiplicative correction could be applied to normalized run to run variation. These data indicate that this could routinely be accomplished in the future through the incorporation of a standard tissue sample in each run.

The N-Glycan Mass Matching is Very Precise and Consistently Accurate Between Runs.

Routine accurate mass identification of N-Glycans from MALDI-MS data has been a common practice since 2008 (16). Orthogonal chemical (amidation, **Figure 2**) and enzymatic (**Figure 3**) strategies have demonstrated the specificity and accuracy of predicted structures without the need for MS/MS (i.e., mass spectrometry fragmentation) approaches. To complement this and more closely investigate our replicate analysis here we queried mass spectra peak-level data for mass (i.e., m/z) variation in matching to one another and the theoretical database.

The standard search mass accuracy window for our N-glycan workflow is 20 ppm (parts per million, or 0.002 parts in 1000. This is already a stringent search window for an accurate mass match based on MALDI-MS. Zooming in on the matched glycan peaks for the replicate analysis here (**Figure 8**) we see that the m/z peaks for the candidate glycoform at 1077.3 m/z match almost identically, well within the 20ppm window (pink highlight). In fact, the mass accuracy of all the matched peaks for this replicate study were 8.9 ppm across all samples (*not shown*). Altogether, the high mass accuracy of matching combined with the relative signal reproducibility between independent replicates, makes this an ideal assay for biomarker discovery in archival tissue samples.

References.

1. West CA, Lu X, Grimsley G, Norris-Caneda K, Mehta AS, Angel PM, Drake RR. Optimization of Multiple Glycosidase and Chemical Stabilization Strategies for N-Glycan Isomer Detection by Mass Spectrometry Imaging in Formalin-Fixed, Paraffin-Embedded Tissues. Methods Mol Biol. 2021;2271:303-316. doi: 10.1007/978-1-0716-1241-5_21. PMID: 33908016.

2. Blaschke CRK, Black AP, Mehta AS, Angel PM, Drake RR. Rapid N-Glycan Profiling of Serum and Plasma by a Novel Slide-Based Imaging Mass Spectrometry Workflow. *Journal of the American Society For Mass Spectrometry*. PMID 32809822 DOI: 10.1021/Jasms.0C00213

3. West CA, Liang H, Drake RR, Mehta AS. A New Enzymatic Approach to Distinguish Fucosylation Isomers of N-linked Glycans in Tissues Using MALDI Imaging Mass Spectrometry. *Journal of Proteome Research*. PMID 32441096 DOI: 10.1021/Acs.Jproteome.0C00024

4. Drake RR, McDowell C, West C, David F, Powers TW, Nowling T, Bruner E, Mehta AS, Angel PM, Marlow LA, Tun HW, Copland JA. Defining the Human Kidney N-Glycome in Normal and Cancer Tissues Using MALDI Imaging Mass Spectrometry. *Journal of Mass Spectrometry : Jms*. e4490. PMID 31860772 DOI: 10.1002/Jms.4490

5. Black AP, Angel PM, Drake RR, Mehta AS. Antibody Panel Based N-Glycan Imaging for N-Glycoprotein Biomarker Discovery. *Current Protocols in Protein Science*. 98: e99. PMID 31721442 DOI: 10.1002/Cpps.99

6. Scott DA, Drake RR. Glycosylation and its implications in breast cancer. *Expert Review of Proteomics*. PMID 31314995 DOI: 10.1080/14789450.2019.1645604

7. Black A, Liang H, West CA, Wang M, Herrera H, Haab B, Angel PM, Drake RR, Mehta A. A Novel Mass Spectrometry Platform for Multiplexed N-glycoprotein Biomarker Discovery

from Patient Biofluids by Antibody Panel Based N-glycan Imaging. *Analytical Chemistry*. PMID 31177770 DOI: 10.1021/Acs.Analchem.9B01445

8. Scott DA, Norris-Caneda K, Spruill L, Bruner E, Kono Y, Angel PM, Mehta AS, Drake RR. Specific N-Linked Glycosylation Patterns in Areas of Necrosis in Tumor Tissues. *International Journal of Mass Spectrometry*. 437: 69-76. PMID 31031563 DOI: 10.1016/J.Ijms.2018.01.002

9. Scott DA, Casadonte R, Cardinali B, Spruill L, Mehta AS, Carli F, Simone N, Kriegsmann M, Mastro LD, Kriegsmann J, Drake RR. Increases in Tumor N-glycan Polylactosamines Associated with Advanced HER2 Positive and Triple Negative Breast Cancer Tissues. *Proteomics. Clinical Applications*. e1800014. PMID 30592377 DOI: 10.1002/Prca.201800014

10. Drake RR, West CA, Mehta AS, Angel PM. MALDI Mass Spectrometry Imaging of N-Linked Glycans in Tissues. *Advances in Experimental Medicine and Biology*. 1104: 59-76. PMID 30484244 DOI: 10.1007/978-981-13-2158-0_4

11. West CA, Wang M, Herrera H, Liang H, Black A, Angel PM, Drake RR, Mehta AS. N-linked glycan branching and fucosylation are increased directly in hepatocellular carcinoma tissue as determined through in situ glycan imaging. *Journal of Proteome Research*. PMID 30110170 DOI: 10.1021/Acs.Jproteome.8B00323

12. Drake RR, Powers TW, Norris-Caneda K, Mehta AS, Angel PM. In Situ Imaging of N-Glycans by MALDI Imaging Mass Spectrometry of Fresh or Formalin-Fixed Paraffin-Embedded Tissue. *Current Protocols in Protein Science*. e68. PMID 30074304 DOI: 10.1002/Cpps.68

13. Angel PM, Mehta A, Norris-Caneda K, Drake RR. MALDI Imaging Mass Spectrometry of N-glycans and Tryptic Peptides from the Same Formalin-Fixed, Paraffin-Embedded Tissue Section. *Methods in Molecular Biology (Clifton, N.J.)*. PMID 29058228 DOI: 10.1007/7651_2017_81

14. Drake RR, Powers TW, Jones EE, Bruner E, Mehta AS, Angel PM. MALDI Mass Spectrometry Imaging of N-Linked Glycans in Cancer Tissues. *Advances in Cancer Research*. 134: 85-116. PMID 28110657 DOI: 10.1016/Bs.Acr.2016.11.009

15. Powers TW, Neely BA, Shao Y, Tang H, Troyer DA, Mehta AS, Haab BB, Drake RR. MALDI imaging mass spectrometry profiling of N-glycans in formalin-fixed paraffin embedded clinical tissue blocks and tissue microarrays. *Plos One*. 9: e106255. PMID 25184632 DOI: 10.1371/Journal.Pone.0106255

16. Ceroni A, Maass K, Geyer H, Geyer R, Dell A, Haslam SM. GlycoWorkbench: a tool for the computer-assisted annotation of mass spectra of glycans. J Proteome Res. 2008 Apr;7(4):1650-9. doi: 10.1021/pr7008252. Epub 2008 Mar 1. PMID: 18311910.

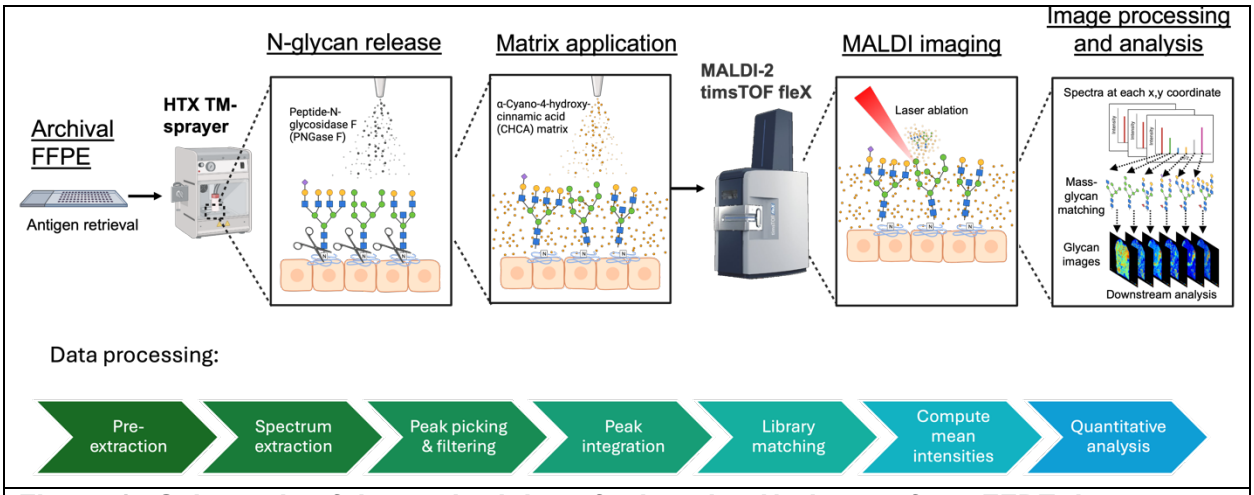

Figure 1. Schematic of the methodology for imaging N-glycans from FFPE tissues. Prior to enzyme application, FFPE blocks are cut at 5 µm, incubated, deparaffinized and undergo antigen retrieval. PNGaseF is then applied, and the slide is incubated before MALDI-IMS. The resulting m/z N-glycan peaks are extracted with integrated intensity and mass matched to a theoretical N-Glycan peak library (16) with an accuracy of 10ppm or better. The data is then linked with histopathology either on the same tissue slice or a serial tissue slice.

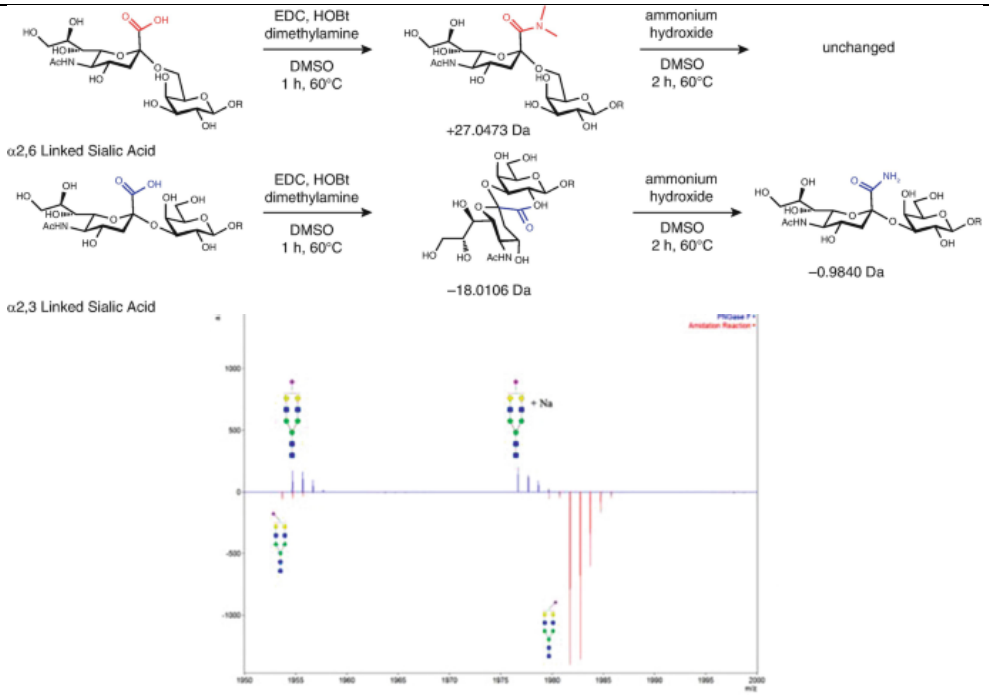

Figure 2. Reaction schematic for amidation–amidation chemical derivatization – confirmation of sialic acids in glycan structure. (*Top*) Schematic of sialic acid derivatization via amidation–amidation reaction. Top: reaction scheme for α2,6 linked sialic acids; Bottom: reaction scheme for α2,3 linked sialic acids. Changes in mass are shown following each step in reaction scheme. (*Bottom*) Spectra for an Nglycan, Hex5HexNAc4, with and without amidation–amidation. The top spectra in blue represents the nonderivatized N-glycan species, carrying one or two Na ions. The bottom spectra in red shows the mass shift resulting from the amidation derivatization. Sialic acid residues are shown as purple diamonds. Those angled to the left indicate αα2,3 linkage while those angled to the right

represent an αα2,6 linkage. The expected presence of a sialic acid in the structure is predictably shifted by the mass of each amide addition.

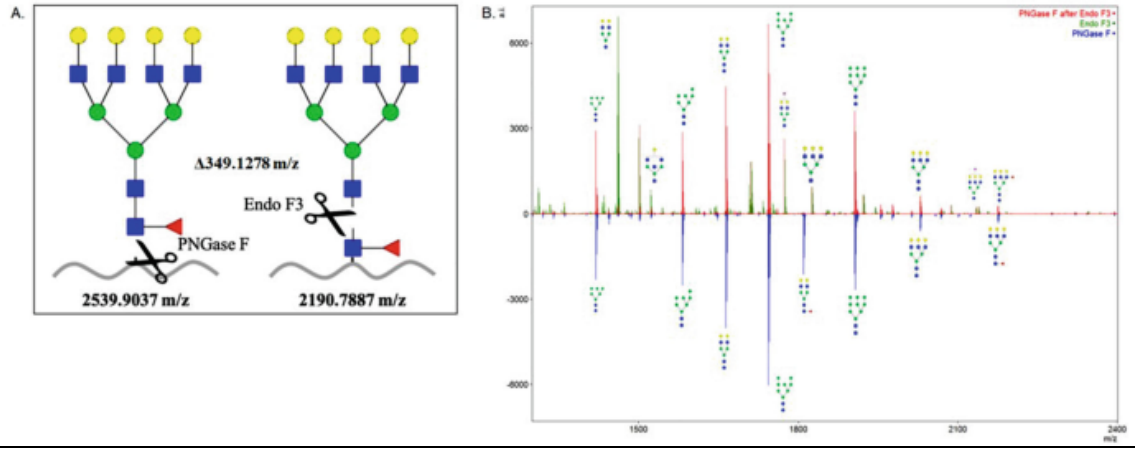

Figure 3. Endoglycosidase F3 cleavage and resulting mass shift structure confirmation. (a) Example of differential cleavage of Endoglycosidase F3 and PNGase F. Endoglycosidase F3 will leave a fucose and *N*-acetylglucosamine residue on the protein, resulting in a −349.1278 *m*/*z* mass shift from the parent *N*-glycan mass. (b) Representative spectra of Endoglycosidase F3 cleaved glycans versus PNGase F cleaved glycans. The use of the Endo F3 results in the expected mass shift as a result of the expected shift in saccharide structure.

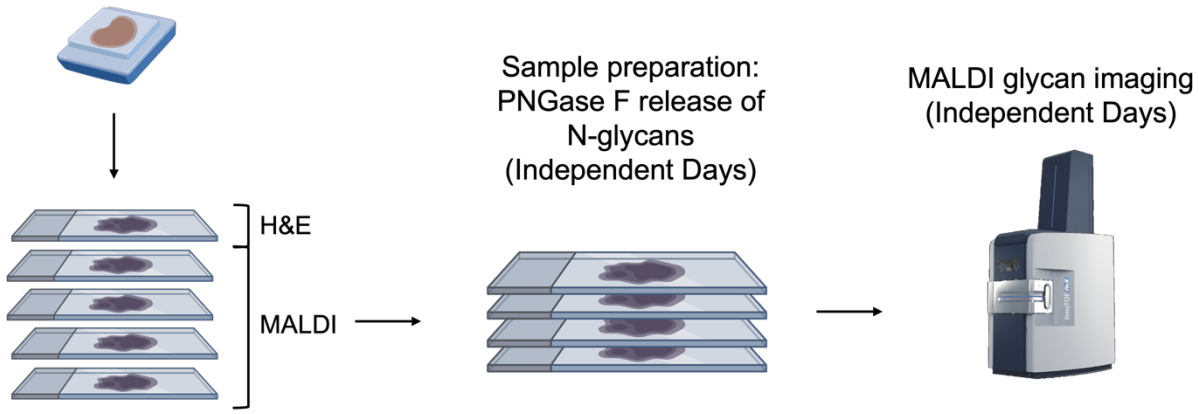

Figure 4. Schematic of the Stanford CIMAC Reproducibility and Robustness Assessment. 5 Serial sections of healthy human kidney were cut onto +glass slides. 1 slide was reserved for H&E staining. The other 4 serial slides were processed for N-Glycan imaging (**Figure 1**) on separate sample preparation and MALDI-imaging days. Kidney was selected for evaluation because of the differential abundance and diversity of glycan structures.

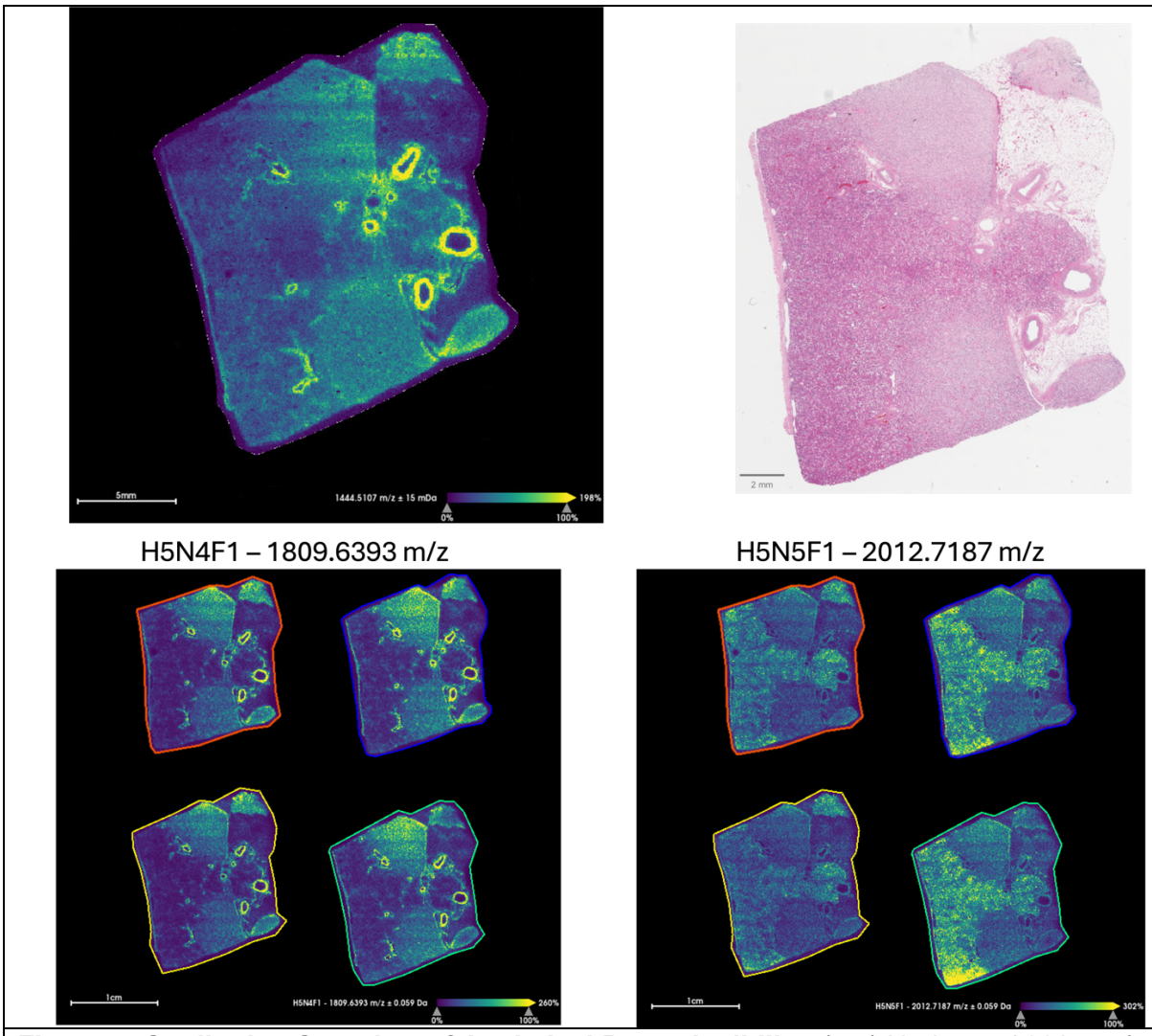

Figure 5. Qualitative Overview of Analytical Reproducibility. (*top*) N-glycan 1444.5 m/z distribution on serial sample 1 compared the adjacent H&E slide stain. (Bottom) Visual comparison of N-Glycan H5N4F1 and H5N5F1 on the 4 kidney serial sections for reproducibility. Intensities are raw / unscaled.

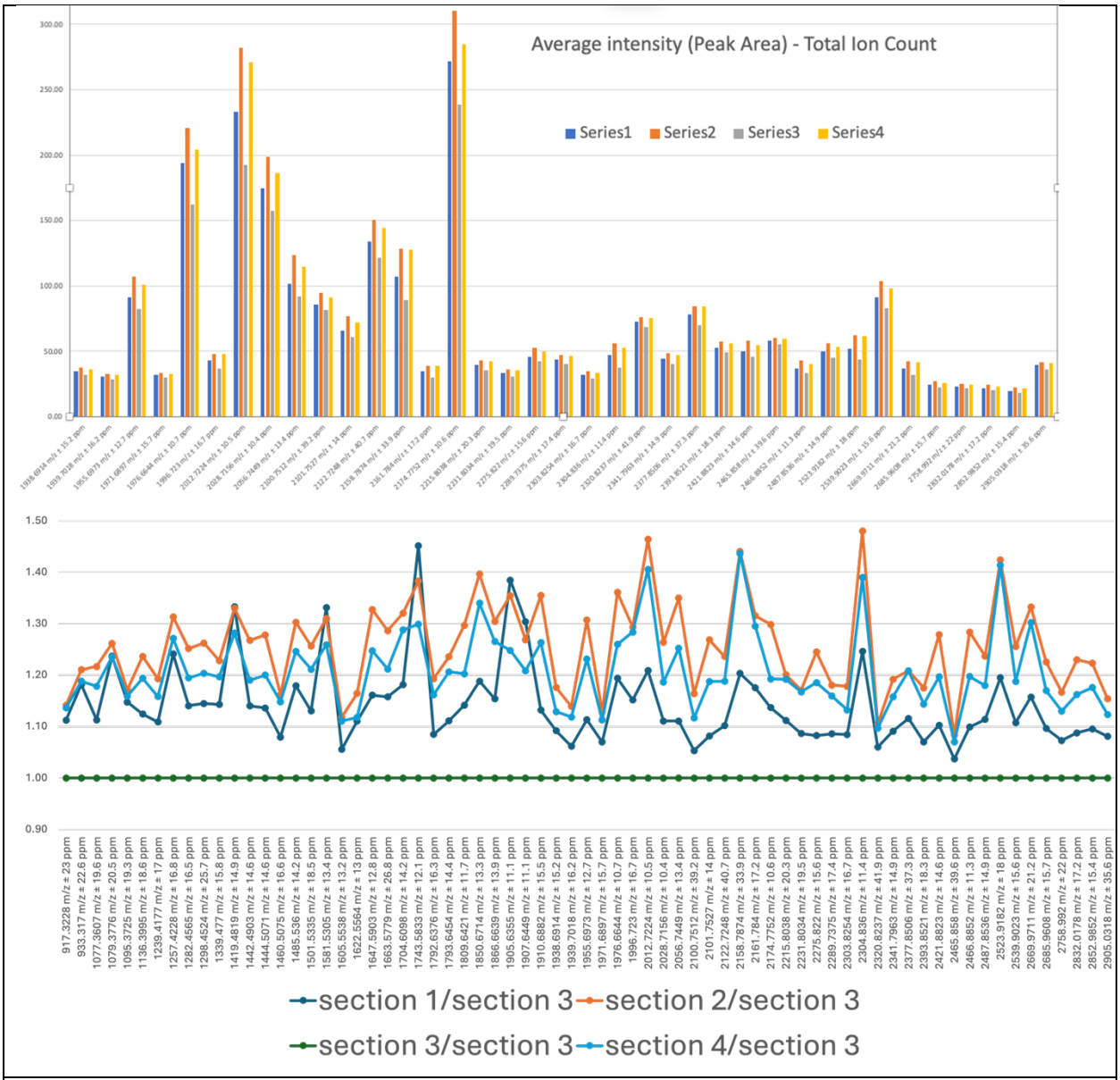

Figure 6. Intensity Variation of MALDI-N-Glycan is Unimodal. Variation in the top expressed glycoforms. (Top) Raw intensities of a subset of matched glycan peaks across the 4 imaging replicates (**Figure 4**). (Bottom) Ratiometric analysis of N-Glycan peak intensities. Absolute intensities of each glycan peak across a given run appear to vary unimodally.

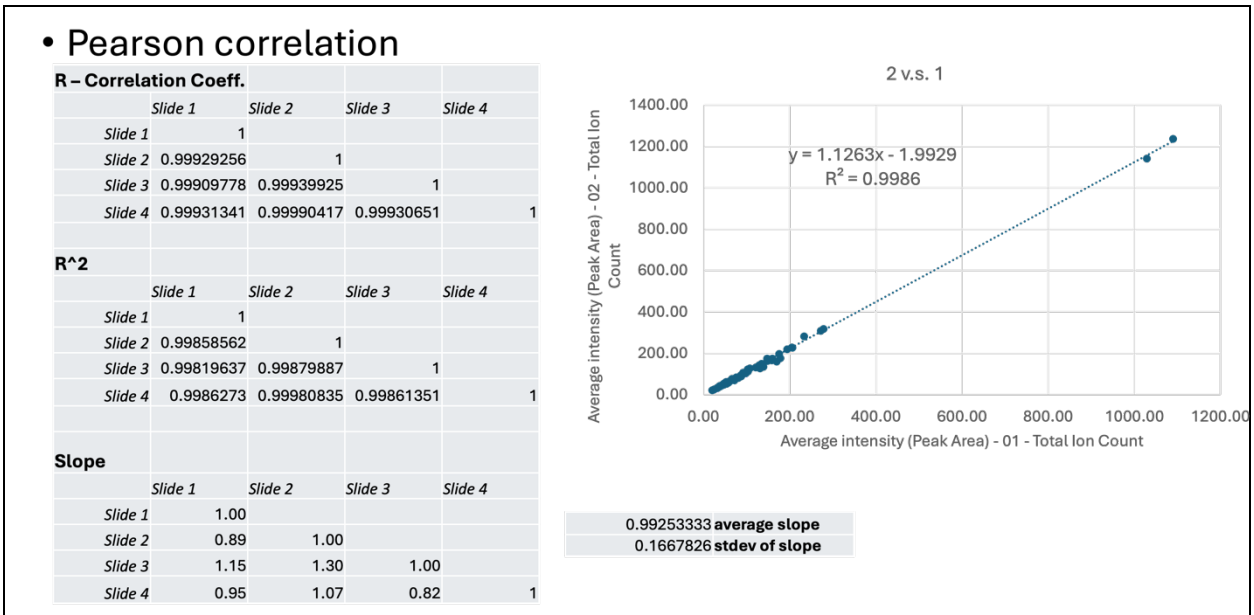

Figure 7. Overall assessment of robustness and reproducibility across 4 independent analytical runs. Comparison of intensities from 270 matched glycan peaks between analytical runs. Left table summarizes the Pearson Correlation Analysis of the 4 replicate slides across one another. Average R^2 correlation is 0.998 with an average slope of 0.99 with an average variance of 14%, reflected **Figure 6**. Right, representative Pearson Correlation plot.

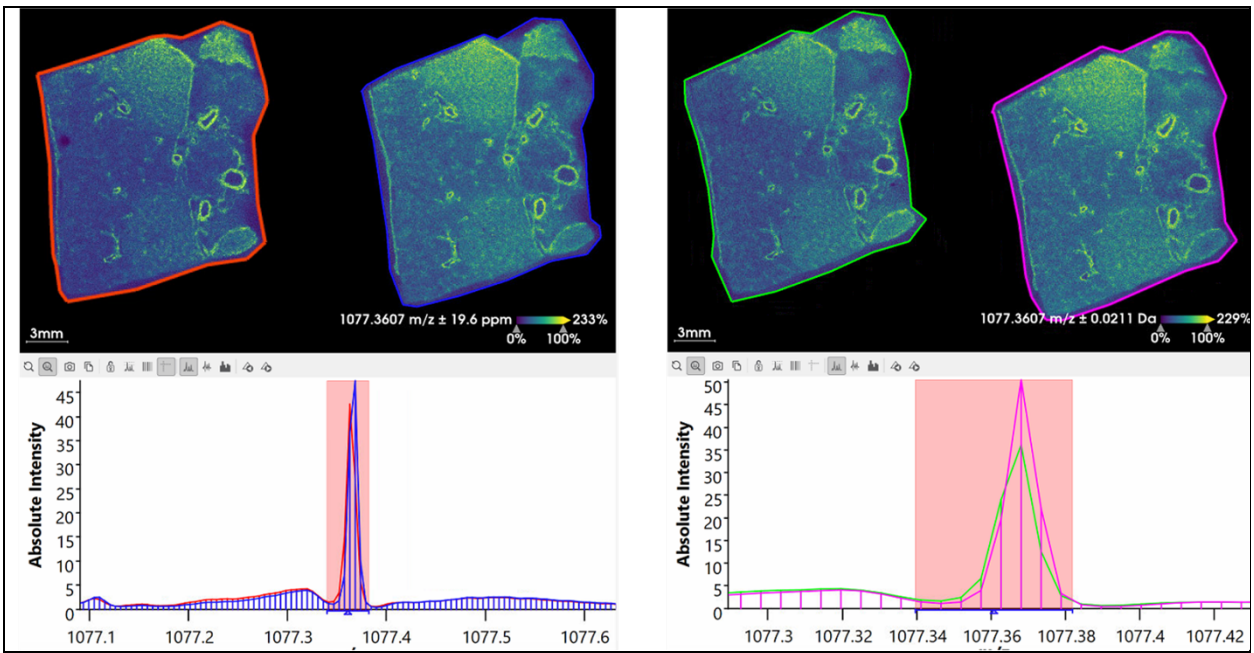

Figure 8. Accuracy and Precision of N-Glycan Mass Matching. Glycan library peaks are assigned with an accuracy of 20ppm (or better). This is 0.002Da per 1000. Shown here is an example of matching spectra for the N-Glycan matched at 1077.3607. *Top* is the map of glycan distribution across 4 samples. *Bottom*, 4 MALDI mass spectra with 20ppm accuracy window (pink).

Appendix I – Stanford MALDI N-Glycan Assay.

Sample Preparation Protocol:
https://dx.doi.org/10.17504/protocols.io.36wgqj2j5vk5/v2

Data Acquisition and Analysis Protocol:
https://doi.org/10.1038/s41467-023-40068-5